Effect of Reflected Waves in SASW Testing of Pavements

J. C. SHEU, K. H. STOKOE II, AND J. M. ROESSET

The Spectral-Analysis-of-Surface-Waves (SASW) method is a rapidly developing in situ seismic method for nondestructively determining Young's modulus profiles of pavement sites. The method is based on the generation and measurement of surface waves (Rayleigh waves). Due to the complex theoretical solution of surface wave propagation in pavements, a multilayered half space with infinite lateral extent has been assumed in the analytical solutions of SASW testing. In addition, only plane surface waves were considered. The existence of direct and reflected body waves and any reflected surface waves, although known to occur in pavements, was neglected in the analytical solutions. To understand the impact of reflected surface waves and direct and reflected body waves in SASW testing, a simplified analytical model was developed. Reflecting boundaries such as edges or joints of a pavement system or the horizontal interfaces between pavement layers were considered. To examine the validity of the model, field tests on a jointed concrete pavement were performed. The results show that reflected surface waves cause fluctuations to occur in the field data (dispersion curves) which would otherwise be a smooth function if only direct surface waves were present. Direct and reflected body waves also create a similar result but to a much lesser extent. Reflected SV-waves (shear waves with vertical particle motion) exhibit the most influence of all direct and reflected body waves, with the effect more important at wavelengths longer than the pavement surface layer. The adverse effect of reflections can be minimized by properly orienting the test array (line passing between the source and receivers) in the field with respect to joints, edges, and cracks in the pavement. For instance, when a vertical reflecting boundary such as a joint is oriented perpendicularly to the SASW array, the adverse effect of reflections can be minimized and nearly eliminated by placing the source between the reflecting boundary and the receivers. When a vertical reflecting boundary such as the pavement edge is near the zone of testing, the effect of reflections can be greatly minimized by orienting the array parallel to and near (about 0.1 times the receiver spacing) the edge.

Nearly all nondestructive testing of pavements involves stress wave propagation. Due to the complex nature of stress wave propagation in pavements, most analytical models are based on the assumption that the seismic waves propagate in a layered half space with no additional boundaries or interfaces. As a result, reflected surface and body waves created by boundaries in the real finite system are not included in these solutions. In fact, whenever a pavement system is tested using a stress wave propagation method, such as the Spectral-Analysis-of-Surface-Waves (SASW) method, reflected waves from discontinuities such as edges, joints, or cracks are inevitably generated. The key reflecting boundaries are nearly always those in the top layer, such as the concrete layer in a rigid pavement.

The existence of reflected surface waves is not considered in the analytical model used to analyze (invert) SASW dispersion curves (*1–3*). Therefore, it is important to investigate how and to what extent reflected waves influence field results (dispersion curves) so that possible errors created by neglecting their existence are not accidentally overlooked. It may then be possible either to avoid or reduce the influence of reflected waves by adjusting the field test procedure and/or in-house data reduction process.

In addition, only plane surface waves are assumed to exist in the inversion process used in the SASW method (*1–3*). However, when the test is carried out in the field, surface waves are generated by applying a point load (impact) on the surface. As a result, body waves (compression and shear) are generated simultaneously with the surface waves. These body waves may propagate directly from the source to the receivers (direct body waves), or they may be reflected, just like surface waves, by discontinuities in the system and then reach the receivers (reflected body waves). The effect of direct and reflected body waves on the dispersion curve is not known and needs to be studied. Sanchez-Salinero et al. (*4*) initiated a formulation which incorporates all waves in the system. However, more work is necessary before this formulation can be easily used and parametric studies can be performed.

A mathematical model which is capable of simulating the effect of direct and reflected body waves and reflected surface waves on dispersion curves in presented herein. Use of this model is first explained with a simple example involving surface waves reflected from the edge of a concrete pavement. To evaluate further the validity of this approach, modeled dispersion curves are compared to actual dispersion curves measured in the field for various locations of pavement joints and edges relative to the general location and orientation of the source and receivers used in SASW testing. Confidence in this model is established with these comparisons, and the model is further used to predict the behavior of dispersion curves for other conditions of interest, such as for the influence of direct and reflected body waves and for multiple reflections of body and surface waves.

BACKGROUND OF SASW METHOD

The SASW method is an in situ seismic method which is used for near-surface profiling of pavement sites. The general

J. C. Sheu, Dames & Moore, 221 Main Street, San Francisco, Calif. 94105. K. H. Stokoe II and J. M. Roesset, Geotechnical Engineering, The University of Texas at Austin, Austin, Tex. 78712.

arrangement of the source, receivers (vertical sensors), and recording equipment is shown schematically in figure 1. The source is a transient vertical impact, often delivered by a hand-held hammer, which generates a group of surface waves with various frequencies. The surface waves travel along the surface in all directions from the source. Two vertical receivers, either geophones or accelerometers, are placed on the surface in a linear array and are used to monitor the propagation of surface wave energy. By analyzing the phase of the cross power spectrum determined between the two receivers, surface wave velocities are determined over the range of frequencies generated. The shear wave velocity profile is then obtained from the surface wave velocities, and finally the Young's modulus profile is determined (*1–4*).

Since the stiffness of a pavement site varies with depth, the velocity of the surface wave becomes a function of wavelength (or frequency). The variation of surface wave velocity with respect to wavelength (frequency) is called a dispersion curve. This dispersive characteristic of Rayleigh (surface) waves is the basis upon which the SASW method is founded. This dispersion curve can be considered the "raw data" collected in the field. The purpose of this paper is to show how joints, edges, and other discontinuities in the pavement system affect the field dispersion curve.

The dispersion curve only represents the relation between surface wave velocity and wavelength. When the medium consists of layers with different stiffnesses (in terms of shear wave velocities or elastic moduli), the relationship between the elastic modulus profile and the field dispersion curve becomes quite complex (*4, 5*). As a result, development of the modulus profile from a measured dispersion curve is one of the key steps in the SASW method. This process, by which the modulus profile is back-calculated from the corresponding field dispersion curve, is called inversion of the dispersion curve (or in short, inversion). However, this aspect of the SASW method (inverting) is not addressed herein because the effects of reflections are more directly seen in the raw data, the measured dispersion curve.

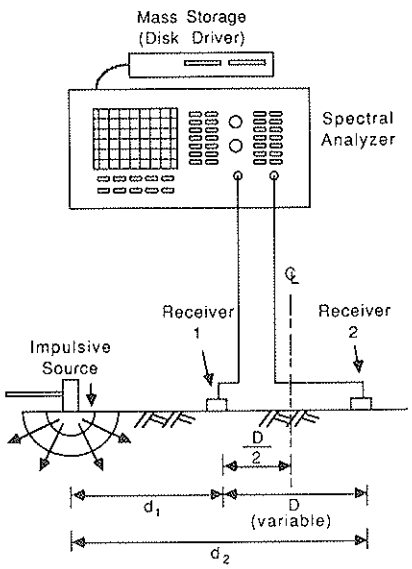

FIGURE 1 Field arrangement of source, receivers, and recording equipment for typical SASW testing.

SIMPLIFIED MATHEMATICAL MODEL

No theoretically complete solution yet exists for wave propagation with vertical, horizontal, and oblique boundaries in a layered system such as a pavement which involves all seismic waves (*6, 7*). In an attempt to simulate wave propagation problems associated with such kinds of systems, a simplified mathematical model was developed. This simplified modeling technique assumes that a true dispersion curve derived solely from direct surface waves is known. The dispersion curve which includes the effects of reflected and/or other direct waves is calculated based on the true dispersion curve by simply adding the influence of any reflected and/or additional direct waves to the true dispersion curve as outlined below.

Imagine that a vertical forcing function is applied at a point on the surface of a layered system, and a pure sine wave with a frequency, f_0, is generated. Two receivers are attached to the surface of the layered system and aligned with the point source to form a linear array (straight line connects source and all receivers) as in SASW testing. The receivers are used to track vertical surface motion. Direct surface waves propagate along the surface in all directions from the source. In addition, reflected waves are created due to the existence of discontinuities in the layered system. As a result, surface (vertical) motion detected by the two receivers is a combination of direct (surface and/or body) waves and reflected (surface and/or body) waves.

Schematic representations of the time records of each receiver are shown in figure 2. Suppose time signals detected by the two receivers after the surface is excited by this point-forcing function are represented by $g(t)$ and $h(t)$, respectively. Then $g(t)$ and $h(t)$ can be expressed by

$$g(t) = \sum_p a_{1p} \sin 2\pi f_0(t - t_{1p}) \tag{1}$$

$$h(t) = \sum_q a_{2q} \sin 2\pi f_0(t - t_{2q}) \tag{2}$$

in which a_{1p} and a_{2q} are amplitudes of various wave arrivals measured by the first and second receivers, respectively, and t_{1p} and t_{2q} are the times of the various wave arrivals at the first and second receivers, respectively. The definitions of a's and t's are shown schematically in figure 3. In the above and following equations, the subscripts are used to denote a specific wave arrival at a particular receiver. The first subscript is used to demote the receiver number, and the second subscript is used to denote the number of the wave arrival. For example, a_{23} represents the amplitude recorded by the second receiver of the third wave arrival (which could be a direct or reflected wave).

Let $G(f)$ and $H(f)$ be the Fourier transforms of $g(t)$ and $h(t)$, respectively. The transforms can then be expressed as

$$G(f) = \sum_p a_{1p} \exp(-i\,2\,\pi\,f_0\,t_{1p}) \quad \text{for } f = f_0 \tag{3a}$$

$$G(f) = 0 \quad \text{for } f \neq f_0 \tag{3b}$$

and

$$H(f) = \sum_q a_{2q} \exp(-i\,2\,\pi\,f_0\,t_{2q}) \quad \text{for } f = f_0 \tag{4a}$$

$$H(f) = 0 \quad \text{for } f \neq f_0 \tag{4b}$$

The cross power spectrum, G_{yx}, for this pair of time signals

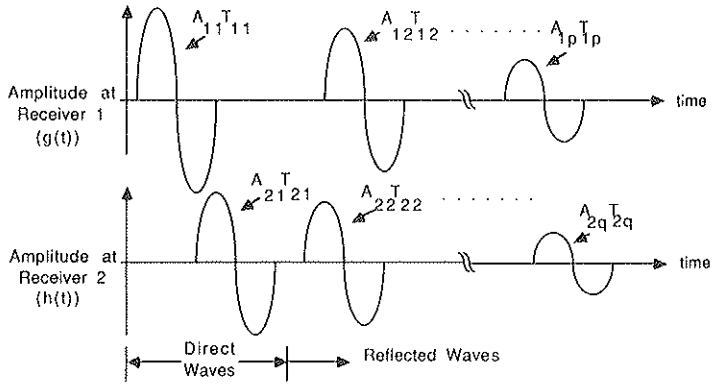

FIGURE 2 Representation of time domain records received by each receiver in SASW testing illustrating combined direct and reflected (packets of energy) waves.

is defined as

$$G_{yx} = G^* \times H \tag{5}$$

in which G^* denotes the complex conjugate of G. The phase of the cross power spectrum at frequency f_0, $\phi(f_0)$, is

$$\phi(f_0) = \text{Tan}^{-1}\left[\frac{\sum_p \sum_q a_{1p}a_{2q} \sin 2\pi f_0(t_{1p} - t_{2q})}{\sum_p \sum_q a_{1p}a_{2q} \cos 2\pi f_0(t_{1p} - t_{2q})}\right] \tag{6}$$

This phase is the key variable used to calculate wave velocity.

In a real SASW test, a wide range of frequencies is generated simultaneously by applying a vertical impact on the surface of the system. As a result, each arrival is no longer a single-frequency arrival but contains a certain range of frequencies. Since equations 1 through 6 were derived with the consideration of only a single frequency, the following modifications are made so that they can be applied to the multiple-frequency condition. Assume while f_0 varies over a range of frequencies generated by the vertical impact, values of a_{1p}, a_{2q}, t_{1p}, t_{2q} vary accordingly. Let A_{1p}, A_{2q}, T_{1p}, and T_{2q} be the amplitude and time functions of frequency at receivers 1 and 2, respectively. Therefore, the functions can be written as

$$A_{1p}(f) = a_{1p}(f_1) + a_{1p}(f_2) + a_{1p}(f_3) + \ldots \tag{7}$$

$$A_{2q}(f) = a_{2q}(f_1) + a_{2q}(f_2) + a_{2q}(f_3) + \ldots \tag{8}$$

$$T_{1p}(f) = t_{1p}(f_1) + t_{1p}(f_2) + t_{1p}(f_3) + \ldots \tag{9}$$

$$T_{2q}(f) = t_{2q}(f_1) + t_{2q}(f_2) + t_{2q}(f_3) + \ldots \tag{10}$$

in which the notations for each subscript of T's and A's, as well as t's and a's, are the same as previously defined and frequencies f_1, f_2, f_3, and so forth are the desired modeling frequencies. Hence, equation 6 can be rewritten as

$$\phi(f) = \text{Tan}^{-1}\left\{\frac{\sum_p \sum_q A_{1p}(f)A_{2q}(f) \sin 2\pi f[T_{1p}(f) - T_{2q}(f)]}{\sum_p \sum_q A_{1p}(f)A_{2q}(f) \cos 2\pi f[T_{1p}(f) - T_{2q}(f)]}\right\} \tag{11}$$

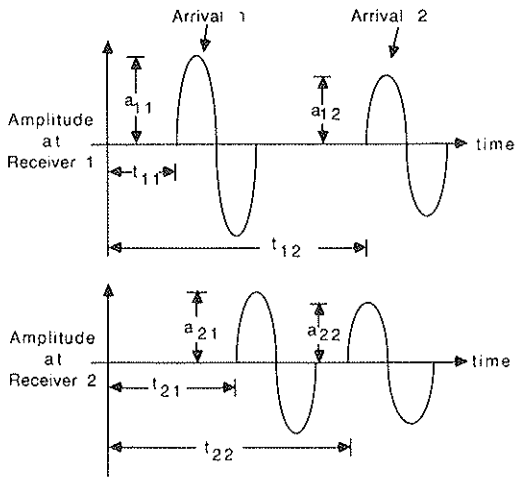

FIGURE 3 Representation of amplitudes (a's) and arrival times (t's) for two single-wave arrivals at each receiver.

Each A, with two subscripts, is a series of amplitudes which are a function of frequency and correspond to the particular arrival denoted by the subscripts. The absolute value of A actually represents the amplitude of the linear spectrum for this particular arrival. Each T, with two subscripts, is a series of travel times which are a function of frequency and correspond to the particular arrival denoted by the subscripts. It is necessary to note that the connotation of "arrival" used in equation 6 is somewhat different than that used in equation 11. In equation 6, each "arrival" has energy at only one frequency. On the other hand, in equation 11, each "arrival" represents a packet of energy containing a range of frequencies. Since equation 6 is a special case of equation 11 and the latter was used for all studies, the second connotation of "arrival," namely a packet of energy over a range of frequencies, is used herein.

It is important to notice that both T's and A's are functions of frequency, and each arrival has its own T and A. Since T is directly related to the arrival times of different frequencies forming the arrival of a particular packet of energy, dispersive characteristics (that is, waves corresponding to different frequencies traveling at different velocities) of this particular

arrival can be accurately modeled by using the proper travel time in "T" for each frequency. In addition, since the arrival of each packet of energy has its own T, waves with different dispersive characteristics can be analyzed together; that is to say, each arrival could have its own dispersion curve. A typical need of modeling waves with more than one type of dispersive characteristic is in the case when combined surface wave and body wave effects are considered. Examples of this type of modeling are illustrated in the following sections.

The amplitude of the linear spectrum, A, for the arrival of each impulse (packet of energy) is simply a measure of the amplitudes of the different frequencies transmitted by this packet of energy. Therefore, the value of A is directly related to the damping characteristics and reflection coefficients of the system being tested. Due to the fact that the arrival of each impulse has its own A, amplitudes of different frequencies which attenuate at different rates can be modeled by using different ratios of amplitudes between different arrivals of the impulse at different frequencies.

In the present inversion process in SASW testing, it is assumed that only plane surface waves exist (*4–6*). As a result, it is implicitly assumed that only one surface wave arrival is detected by the receivers. Let T_{11} and T_{21} be the arrival times of this direct surface wave at each receiver. The corresponding phase of the cross power spectrum, $\phi(f)$, can be expressed as

$$\phi(f) = 2\pi f[T_{11}(f) - T_{21}(f)] \tag{12}$$

Equation 12 is just a special case of equation 11 with p and q both equal to 1. Also notice that in equation 11, it is not necessary to have T_{11}, T_{21}, A_{11}, and A_{21} associated with the arrival of the direct surface wave. In fact, arrivals in equation 11 can be considered in any random order. However, to avoid any possible confusion, T_{11}, T_{21}, A_{11}, and A_{21} are used to represent only direct surface wave arrivals for all discussions presented hereafter.

The problem faced in typical SASW testing in terms of reflections is now clear. In the field, measured phases of cross power spectra are in the fashion of equation 11, but during the in-house inversion stage, the phases of cross power spectra are assumed to be in the fashion of equation 12. The difference between these two equations is the error introduced by waves other than the direct surface wave. As such, it is possible to study the influence of reflected and direct waves on field dispersion curves by using equations 11 and 12, as shown in the following sections.

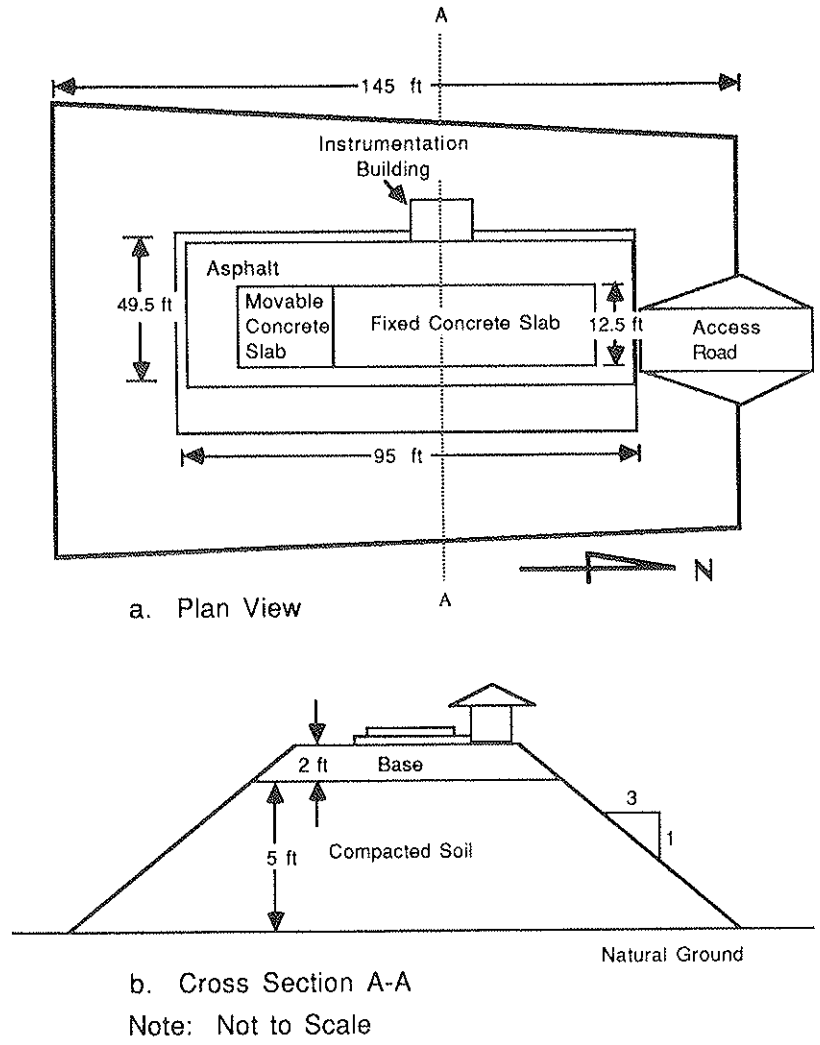

FIGURE 4 Plan and cross-sectional views of BRC pavement facility.

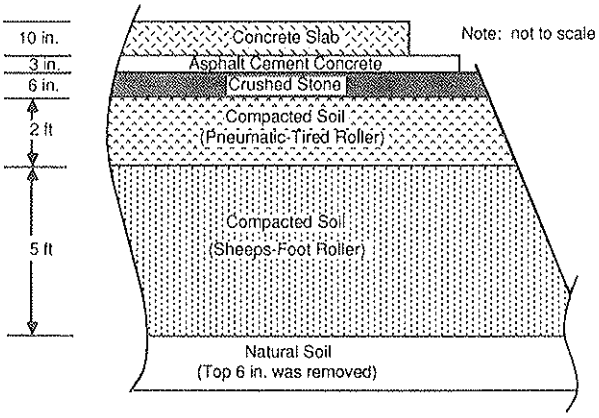

FIGURE 5 Material profile at BRC pavement facility.

FIELD TESTING

To investigate the validity of the simplified mathematical model, field tests were performed. All field data referred to in this work are from tests performed on the jointed concrete pavement at the research facility at Balcones Research Center (BRC), The University of Texas at Austin. This research facility was designed for the study of nondestructive pavement evaluation devices such as the SASW, Dynaflect, and falling weight deflectometer devices (*8*). A schematic of the BRC facility is shown in figure 4, and the material profile at the facility is presented in figure 5.

A Hewlett Packard model 3562A dynamic signal analyzer was used in the field for data collection, mainly phases of the cross power spectrum and coherence functions (*3, 9, 10*). Different types of accelerometers and geophones were used to monitor motions on the pavement surface. Most field data, however, were collected using PCB model 308B02 accelerometers as motion monitoring devices. Field data (phases of cross power spectra) were transferred to a MASSCOMP model MC5500 minicomputer through a general-purpose interface bus for further processing. With the MASSCOMP computer, the user is able to filter out low quality and questionable phase information acquired in the field, calculate the dispersion curves from the filtered phase information, average the dispersion curves from different receiver spacings to find the final (averaged) dispersion curves, and perform other miscellaneous plotting and numerical manipulations.

SIMPLE EXAMPLE

A simple example is given here to illustrate the use of the equations and procedures outlined above. This example models a field test performed at the BRC facility on January 3, 1986. The test was performed on the north end of the fixed concrete slab. A detailed layout of this test is shown in figure 6. Three nearby reflecting boundaries are denoted as A, B, and C, as shown in figure 6. Receivers were placed with a 40-foot (122 cm) spacing between them, and each one was 4 feet (122 cm) away from the nearest reflecting boundary. The source was placed at the edge of reflecting boundary A. The existence of reflecting boundary C was neglected in this example.

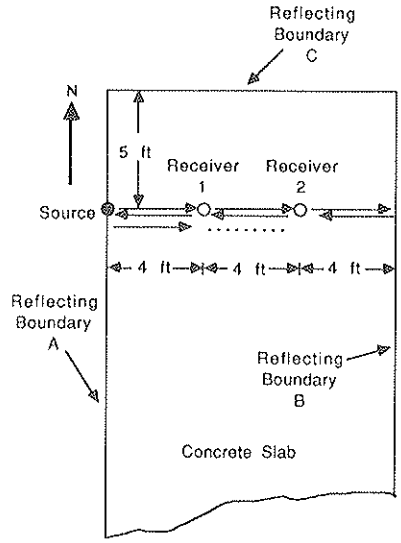

FIGURE 6 Detailed layout of SASW testing used in modeling example.

As soon as a pulse is generated with the source, this pulse starts to travel from the source to receiver 1 and then receiver 2 and finally reaches reflecting boundary B. Before this pulse reaches reflecting boundary B, it is considered as a direct surface wave. After the pulse reaches reflecting boundary B, it will reflect back and ne considered a reflected surface wave from now on. The reflected pulse will travel past receiver 2 and then receiver 1 and finally reach reflecting boundary A. It will then be reflected by boundary A and head towards reflecting boundary B. The pulse will eventually be bounced back and forth by reflecting boundaries A and B until all energy is dissipated. Typical field time records for this site are shown in figure 7. The reflected surface waves detected by each receiver can easily be identified and are indicated by

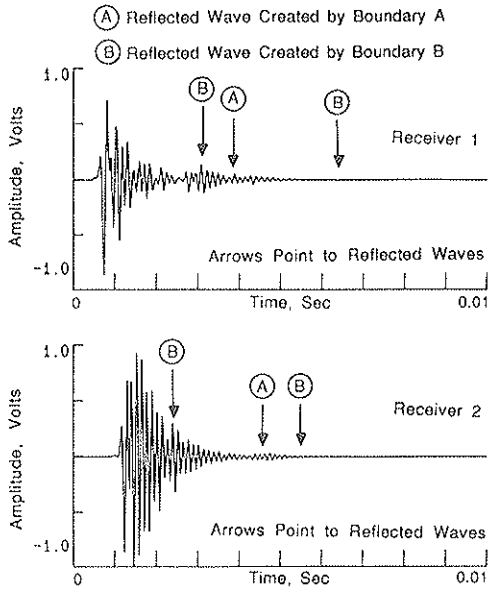

FIGURE 7 Typical time record illustrating the influence of reflected surface waves for test arrangement shown in figure 6.

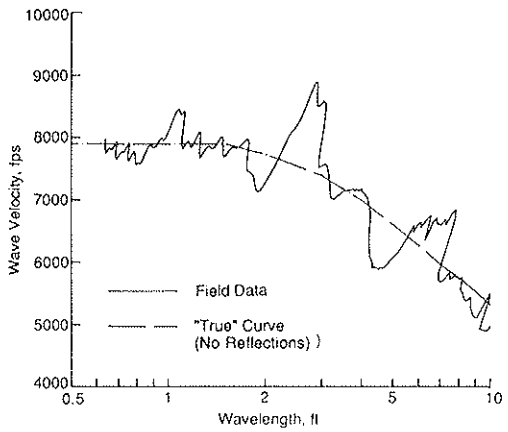

FIGURE 8 Comparison of field (measured) dispersion curve with the dispersion curve ("true") for no reflections for the test arrangement in figure 6.

the arrows shown in the figure. (Of course, there are more reflections than those indicated, but those indicated are the key reflections.)

To simplify this example, the effect of reflecting boundary C is neglected, and only the first reflected surface wave from boundary B is considered. THe measured (field) dispersion curve is shown by the solid line in figure 8. The "true" dispersion curve for this case should look like the smooth, dashed line drawn through the dispersion curve in figure 8. (The "true" dispersion curve is the dispersion curve for only direct surface waves in a layered system with infinite horizontal extent.) From figure 6, the distances that a direct pulse travels from the source to receivers 1 and 2 are 4 and 8 feet (122 and 244 cm), respectively. Since the "true" dispersion curve is known (figure 8), $T_{11}(f)$, $T_{21}(f)$ and "true" phase corresponding to each frequency can be calculated. The "true" phase derived from this "true" dispersion curve is shown in figure 9a, and the corresponding "true" dispersion curve (which has been shown in figure 8) is shown in figure 9b.

Notice that although there is a significant wave velocity change in the dispersion curve shown in figure 9b at a wavelength of about 1.5 feet (46 cm), the change is barely observable in the phase of the cross power spectrum (corresponding to figure 9a when the frequency is smaller than about 4000 Hz).

From figure 6, the first reflected pulse detected by receiver 1 is the one which travels from the source to reflecting boundary B and then back to receiver 1. The distance of travel for this pulse is 20 feet (6.1 m). By the same token, the first reflected pulse detected by receiver 2 is the one which travels from the source to reflecting boundary B and then back to receiver 2. The distance of travel for this pulse is 16 feet (4.9 m). Based on this information and by assuming that reflected surface waves have the same dispersive characteristics (same dispersion curve shown in figure 9b) as direct surface waves, it is possible to calculate $T_{12}(f)$ and $T_{22}(f)$ at all frequencies for both reflected waves.

Reflecting boundary B represents a free boundary at the edge of the concrete pavement. Therefore, reflected waves should have displacements in phase with direct waves. (All A's should have the same sign.) The amplitudes for each pulse detected by receiver 1, $A_{11}(f)$ and $A_{12}(f)$, are assumed to be

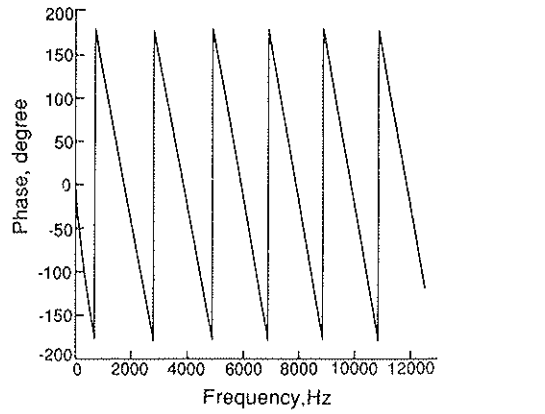

a. Phase of Cross Power Spectrum for 4-ft Receiver Spacing

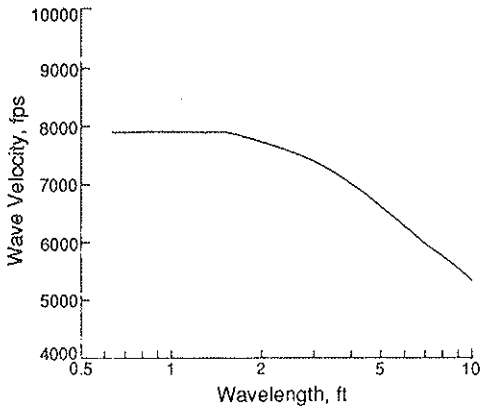

b. Dispersion Curve Associated with Phase Shown Above

FIGURE 9 (a) "True" phase of the cross power spectrum and (b) corresponding "true" dispersion curve for test arrangement shown in figure 6 (only direct surface wave).

1.0 and 0.36, respectively. The amplitudes detected by receiver 2, $A_{21}(f)$ and $A_{22}(f)$, are assumed to be 0.9 and 0.4, respectively. The relative magnitudes of the amplitudes used for the direct and reflected surface waves are more or less in the same order as shown in figure 7. However, it is not correct to use the exact amplitudes measured from the time records shown in figure 7, because reflected waves tend to overlap with the direct waves and with other reflected waves. As a result, their real amplitudes are distorted. All needed information is complete at this point, and the modeled dispersion can be calculated by using equation 11.

Comparison of the modeled and measured phases of the cross power spectrum is shown in figure 10. Comparison of the modeled and field dispersion curves in shown in figure 11. These two comparisons indicated that equation 11 is quite capable of modeling the fluctuations (ripples) that appear in the field data. The amplitudes and locations of the modeled ripples are somewhat different, but are close to the field data. The similarity of modeled and field data give strong support to the modeling process discussed earlier. It also seems that even though the lack of knowledge about amplitudes of all arrivals led to crude estimates of A's in equation 11, the model still generated a dispersion curve which is similar to the field data.

It is also interesting to note that all ripples in the modeled phase (figure 10) have very similar amplitudes, but the ampli-

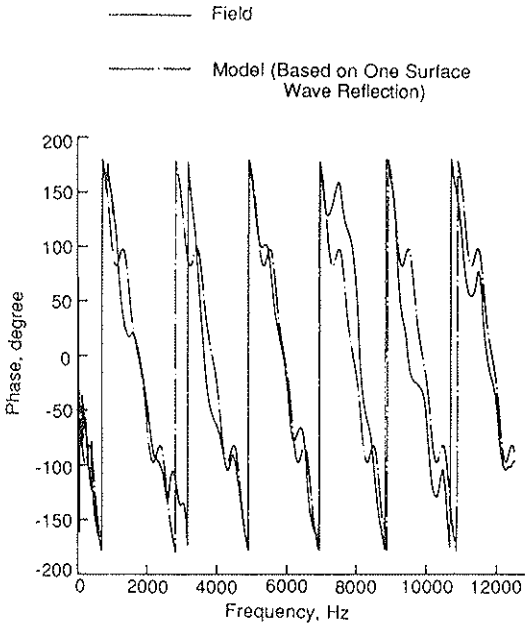

FIGURE 10 Comparison of field and modeled phases of cross power spectra for test arrangement in figure 6.

tudes of the ripples in the dispersion curve (figure 11) have an increasing trend as wavelength increases. This same phenomenon is found in the field data. In fact, experience indicates that this phenomenon commonly exists in most field data. This is due to the fact that when the phase of the cross power spectrum is translated to the dispersion curve, any disturbance in the high frequency range, which corresponds to the short wavelength range, is deamplified. Any disturbance in the low frequency range, on the other hand, corresponds to the long wavelength range and is amplified. As a result, disturbances in the low frequency range cause more problems than disturbances in the high frequency range. In terms of sampling depth, short wavelengths sample shallow depths. Therefore, material properties sampled at shallow depths are less sensitive to disturbances caused by reflected surface or body waves. This material sampling characteristic of the SASW method results in the method being very accurate for measurement of near-surface material properties, such as in the pavement surface layer (*11*).

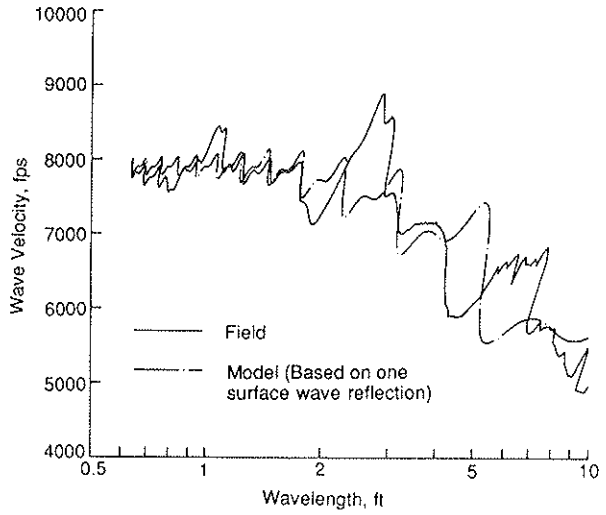

FIGURE 11 Comparison of field and modeled dispersion curves for test arrangement in figure 6.

REFLECTED SURFACE WAVES

The study of reflected surface waves was divided into three major subjects: (1) the effect of reflected surface waves from a vertical reflecting boundary oriented perpendicularly to the source/receiver array, (2) the effect of reflected surface wave from a vertical reflecting boundary oriented parallel to the source/receiver array, and (3) the effect of the distance between a vertical reflecting boundary and the source/receiver array. Model and experimental studies were performed on all subjects, with the exception that a model study was not performed on the effect of distance between the source/receiver array and a vertical reflecting boundary oriented perpendicularly to this array. This latter problem is directly related to damping (not geometry) in the system and is outside the scope of the simplified mathematical model.

Typical results for the effects of cases 1 and 2 cited above are shown in figures 12 and 13. First, consider the field dispersion curves shown in figures 12 and 13. These curves consist of a basic smooth curve upon which ripples or fluctuations are imposed. In the range of wavelengths shorter than about 0.5 foot (15 cm), this basic curve can be approximated by a horizontal line with an average wave velocity of about 7800 fps (2377 m/s). This average surface wave velocity correctly represents the stiffness of the concrete layer (modulus equal to 5.4×10^6 psi) and shows that the field data should be "smoothed" to eliminate the effect of surface wave reflections.

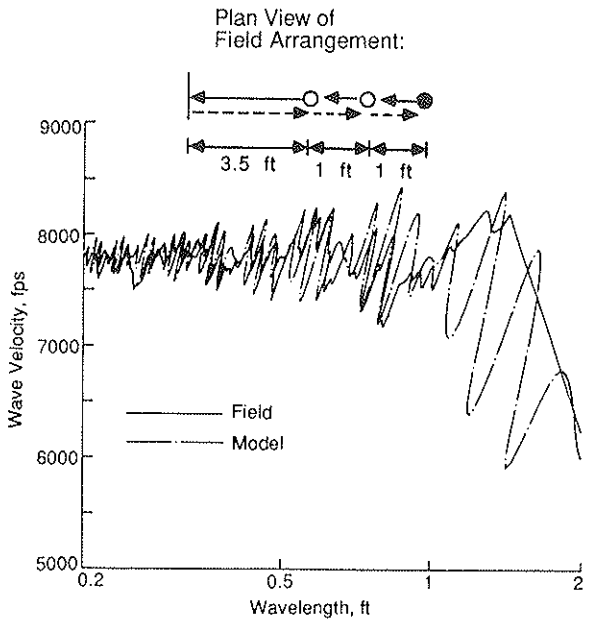

FIGURE 12 Comparison of field and modeled dispersion curves for surface waves reflected from a vertical boundary; receivers placed between source and reflecting boundary.

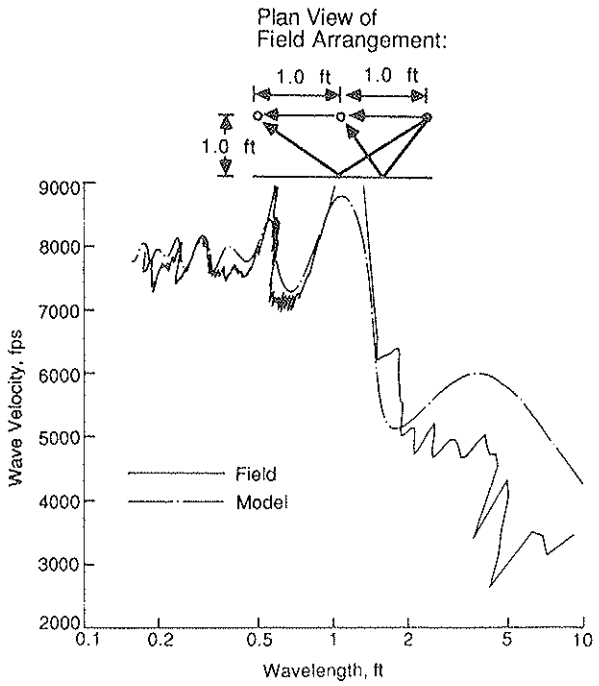

FIGURE 13 Comparison of field and modeled dispersion curves for surface waves reflected from a vertical boundary; test array oriented parallel to reflecting boundary.

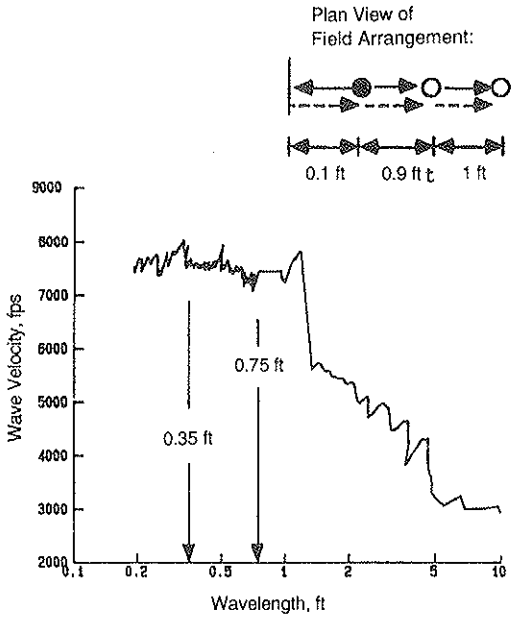

FIGURE 14 Field dispersion curve for surface wave reflected from a vertical boundary; source placed between receivers and reflecting boundary.

Modeled dispersion curves, shown in figures 12 and 13, closely describe the main ripples (fluctuations) present in the field data. It is clear that reflections impose ripples or fluctuations onto the dispersion curves. Although not all peaks and troughs overlap for both curves, the modeled dispersion curve shows the significant characteristics of the fluctuations. Since only one kind of reflected wave with only one reflection is considered in this model, minor discrepancies between the modeled and field data are possibly due to other reflected waves which are not considered in this first approximation model. In addition, uncertainties in estimating amplitudes and times (A's and T's) also introduce some errors into the modeled dispersion curves. However, it is clear that the model is reproducing the general trend and major fluctuations in the field curve. More importantly, the model shows that fluctuations in the field data should be smoothed to represent the theoretical assumption of a multilayered half space with infinite lateral extent.

The model shows that the effects of reflected surface waves from a reflection boundary oriented perpendicularly to the source/receiver array are minimized by placing the source between the boundary and the receivers. When this configuration is used, reflected surface waves travel in the same direction as the direct surface waves, and both the direct and reflected waves can be combined and treated as one direct wave of longer duration. This combination is not possible when the direct and reflected surface waves travel in opposite directions, as occurred in the testing illustrated in figure 12.

Field verification of the beneficial effect of orienting the testing array so that reflected and direct surface waves propagate in the same direction is shown in figure 14. Upon comparison of the field dispersion curves shown in figures 12 and 14, especially in the range of wavelengths from about 0.35 to 0.75 foot (11 to 23 cm), one can see that the amplitudes of the ripples in figure 14 are much smaller than in the case illustrated in figure 12. This result occurs because, for the case shown in figure 12, the reflected surface waves are propagating in the opposite direction to the direct surface waves. Hence, there is an adverse effect on the dispersion curve in figure 12. In the case shown in figure 14, the reflected surface waves are propagating in the same direction as the direct surface waves, and essentially no interference occurs.

The model and experimental studies involving the effect of reflected surface waves from vertical boundaries oriented parallel to the test array also showed that the adverse impact of reflected waves could be minimized by proper placement of the array. As the center line of the SASW array is moved away from the pavement edge, reflected surface waves are increasingly out of phase with respect to direct waves and, hence, have a more adverse effect on the dispersion curves. However, at the same time, the amplitudes of reflected waves decrease with increasing distance from the boundary which reduces the adverse effect on the dispersion curves. The combination of these two effects makes the choice of the best center line location of the array relative to the pavement edge not completely straightforward. Suppose that the source/receiver spacing is defined as D, as shown in figure 15, and the distance between the array and the parallel boundary is $k \times D$. The field and modeled data lead to the conclusion that there are two possible ranges for k which result in minimizing the effect of reflected surface waves. These ranges for k can be expressed as

$$k \geq 3.0 \tag{13}$$

or

$$k \leq 0.2 \tag{14}$$

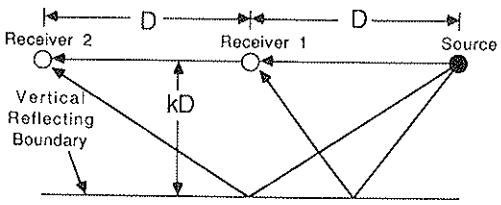

FIGURE 15 Normalized scale illustrating array/boundary configuration for the test array oriented parallel to the reflecting boundary.

Either of these criteria will result in making the influence of reflected surface waves relatively small and can be used as a guide for locating the test array.

DIRECT AND REFLECTED BODY WAVES

Surface impacts, generally from hammers or drop weights, are used to generate surface waves in SASW testing. In addition to generating surface waves, surface impacts also generate unwanted body waves. These body waves reach the receivers either directly or through reflections. Problems arise from the fact that body waves propagate with different velocities and have different dispersive characteristics than surface waves. As a result, body waves can alter the measured dispersion curve adversely.

The adverse impact of body waves on the dispersion curve is expected to be less than the effect of reflected surface waves just shown. This expectation is based on the fact that the energy generated by a vertically oscillating source on the surface of a homogeneous half space is distributed as follows (*12*): 67% in Rayleigh (surface) waves, 26% in shear waves (S-waves), and 7% in compression waves (P-waves). It is clear, therefore, that body waves carry only a small portion of the total energy generated by a surface impact. Furthermore, geometrical damping for body waves in much higher than for surface waves, which means that the negative impact from body waves is further diminished.

There are instances when the boundary which reflects body waves (such as the bottom of the pavement surface layer) is much closer to the test array than the boundary which reflects surface waves. Under these conditions, reflected body waves may become important, and their influence on dispersion curves needs investigation. The effects of body waves on dispersion curves have not been evaluated in the past. Therefore, studies were conducted with the simplified mathematical model in an attempt to identify their influence, to evaluate the severity of their influence, and to provide guidelines for reducing their adverse effects on dispersion curves.

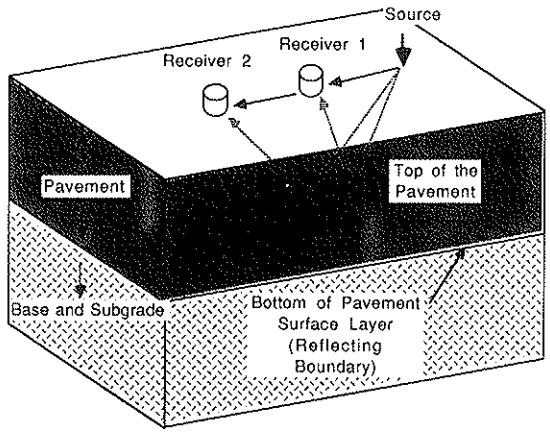

FIGURE 16 Generation of reflected body waves from bottom of concrete slab.

The generation of reflected body waves from the bottom of the pavement surface layer is shown schematically in figure 16. Three kinds of body waves commonly exist in a pavement system: P-waves, SH-waves, and SV-waves. Since both the direction of the impacts and the direction of the receivers are oriented vertically in SASW testing, particle motions in the vertical direction are usually dominant and are best measured. As a result, the influences of direct SV-waves, reflected SV-waves, and reflected P-waves are of the greatest concern. However, in this study, reflected SV-waves were found to be the most important, so only these results are presented herein.

Ray paths of shear waves used in the model simulation are shown in figure 17. Only one reflecting boundary is considered in this study, which is the bottom of the top concrete pavement layer. Because this interface represents a location of significant stiffness change, a fair amount of energy will be reflected by this interface. (An interface with a large stiffness change reflects more energy than an interface with a small stiffness change.) In addition, this interface usually is much closer to the source and receivers than other reflecting boundaries. Therefore, this reflecting boundary was selected for study.

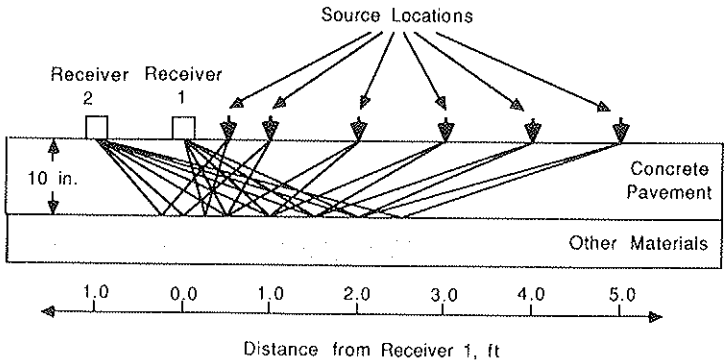

FIGURE 17 Ray paths assumed for body waves reflected from bottom of concrete pavement.

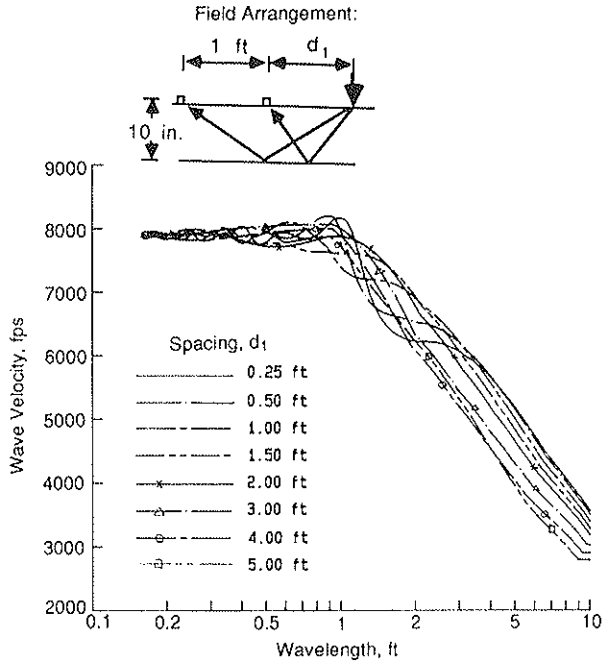

FIGURE 18 Modeled dispersion curves for shear waves reflected from bottom of concrete pavement; fixed receivers spacing of 1 foot and various source-to-receiver distances.

The modeled dispersion curves are shown in figure 18. The amplitudes, A, used for direct surface waves at receivers 1 and 2 are 1.0 and 0.9, respectively, and for reflected shear waves are 0.15 and 0.12, respectively. These amplitudes are used without any change for all cases, so that the effect of source/receiver distance can be more easily identified. Since shear (body) waves attenuate at a much faster rate than surface waves, their effect on the dispersion curves will decrease as the source/receiver distance increases. Therefore, the effect of reflected waves is somewhat overestimated for larger source/receiver spacings in the model.

The modeled dispersion curves shown in figure 18 demonstrate that, as the source/receiver spacing increases, fluctuations in the dispersion curve decrease. In addition, the shear wave has more influence in the long wavelength range (greater than about 0.7 foot, or 21 cm) than in the short wavelength range. For wavelengths of less than about 0.5 foot (15 cm), the effect is negligible. Since surface waves with wavelengths less than 0.5 foot (15 cm) sample basically the top concrete layer, reflected shear waves barely affect the measurement of material stiffness in the concrete layer, an important observation.

The effects of the direct compression and shear waves, as well as reflected compression waves, were much less than that shown in figure 18, and, therefore, are not shown here. A relative comparison of the effect on dispersion curves of reflected body waves versus reflected surface waves is illustrated in figure 19. The effect of body waves reflections, shown in figure 19a, is not nearly as important as the effect of a single surface wave reflection (for the case of a reflected surface wave propagating in the opposite direction to the direct surface wave) which is imposed on the body wave reflections in figure 19b. As such, one can see that reflected surface waves can cause the bulk of the fluctuations in the measured dispersion curves in these tests. Body waves only contribute more at wavelengths greater than the concrete slab thickness.

SUMMARY AND CONCLUSIONS

Seismic wave propagation methods, such as the SASW method, have proven through the years to be powerful methods for assessing moduli profiles. The nondestructive and easy-to-apply nature of the SASW method has made this technique attractive to engineers. Significant theoretical and practical advances in the SASW method have occurred in the past few years, and this method is rapidly becoming an important method for nondestructive testing of pavement systems.

An investigation of the adverse effects of reflected surface waves and direct and reflected body waves on field dispersion curves, the "raw data" of the SASW method, is presented. A simplified mathematical model to account for these effects is given. Field measurements were performed at the rigid pavement facility at Balcones Research Center to compare with the model. The usefulness of the model is confirmed by the good agreement between modeled and field dispersion curves. In the past, it was a puzzle to determine if the fluctuations in dispersion curves were really caused by fluctuations in the material properties or whether there were some other explanations. In this study, it is found that the reflected waves can impose ripples (fluctuations) onto the "true" dispersion curves. If the effect of reflected waves on the dispersion curves is removed, the dispersion curve is basically a smooth curve. At most pavement sites, the dispersion curve corresponding to short wavelengths (about equal to the thickness of the top layer and less) is very flat and close to a straight line, which indicates that the material property in the top pavement layer is usually very uniform.

Based on both model and field studies, it is concluded that the adverse effects from reflected surface waves upon dispersion curves can be reduced by proper arrangement of the source and receiver relative to the boundary. In the case when the vertical reflecting boundary is oriented perpendicularly to the test array, the adverse effect of reflected waves can be reduced to a minimum by placing the source between the reflecting boundary and the receivers. In the case when the reflecting boundary is oriented parallel to the test array, it is better to have the test array located either very close to the reflecting boundary, so that reflected surface waves are very much in phase with the direct surface waves, or as far as possible from the reflecting boundary, so that the amplitudes or reflected surface waves are relatively low compared to the direct surface waves.

Direct and reflected body waves were also studied with the analytical model. Reflected body waves are more important than direct body waves in the top pavement layer and result from reflections at the interfaces at the top and bottom of this layer. As shown in this study, body waves also cause fluctuations in the field dispersion curve, but to a much lesser extent than reflected surface waves.

ACKNOWLEDGMENTS

The project was sponsored by the Texas State Department of Highways and Public Transportation, whose support is

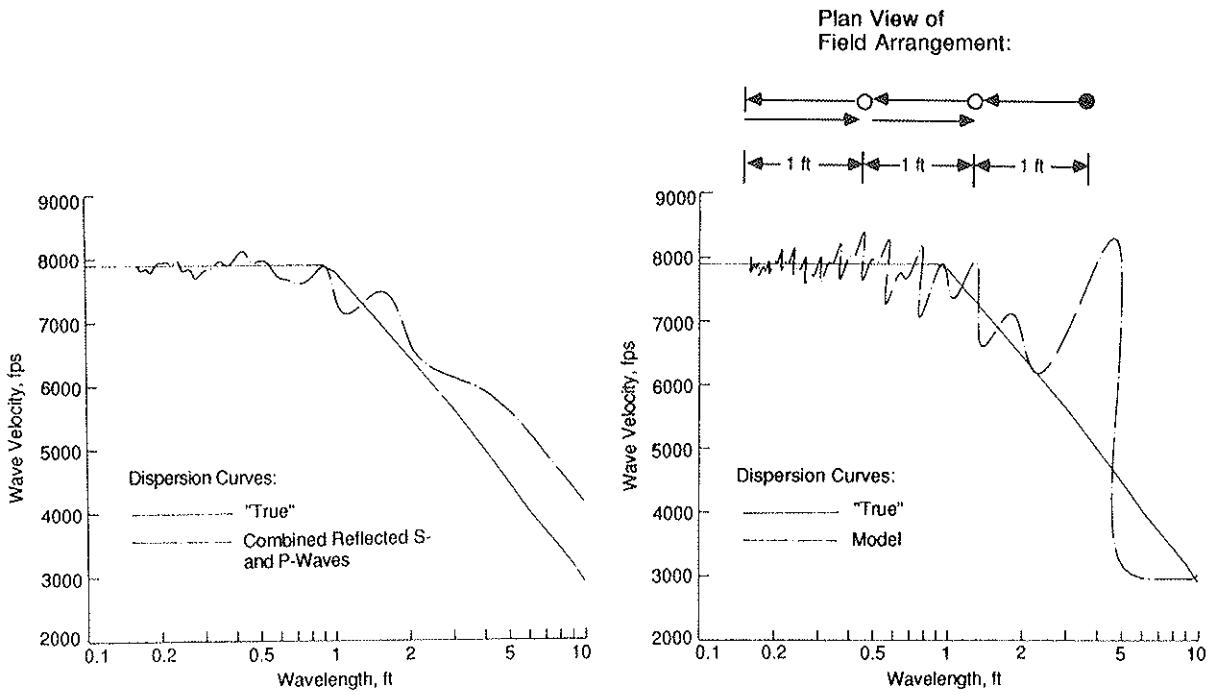

a.) Modeled Dispersion Curve with Combined Reflected S-Waves and Reflected P-Waves.

b.) Modeled Dispersion Curve with Combined Effect from Body Wave Reflections and Reflected Surface Wave.

FIGURE 19 Comparison of the relative effect of reflected body waves versus reflected surface waves on dispersion curves.

gratefully acknowledged. The encouragement and helpful suggestions of R. Briggs and R. Rogers of that department and the constructive discussions and guidance of S. Nazarian, I. Sanchez-Salinero and G. Rix of The University of Texas are sincerely appreciated.

REFERENCES

1. S. Nazarian and K. H. Stokoe, II. In Situ Determination of Elastic Moduli of Pavement Systems by Spectral-Analysis-of-Surface-Waves Method (Practical Aspects). *Research Report 368-1F*. Center for Transportation Research, The University of Texas at Austin, May 1986, 187 pp.
2. S. Nazarian and K. H. Stokoe, II. In Situ Determination of Elastic Moduli of Pavements Systems by Spectral-Analysis-of-Surface-Waves Method (Theoretical Aspects). *Research Report 437-2*. Center for Transportation Research, The University of Texas at Austin, Aug. 1986, 78 pp.
3. S. Nazarian and K. H. Stokoe, II. Use of Surface Waves in Pavement Evaluation. In *Transportation Research Record 1070*, TRB, National Research Council. Washington, D.C., 1986, 39 pp.
4. I. Sanchez-Salinero, E. W. Chang, J. M. Roesset, and K. H. Stokoe, II. Complete Analytical Solution for Wave Propagation in a Layered System, *Research Report 1123-1*. Center for Transportation Research, The University of Texas at Austin (in press).
5. S. Nazarian. *In Situ Determination of Elastic Moduli of Soil deposits and Pavement Systems by Spectral-Analysis-of-Surface-Waves Method*. Ph.D. dissertation. The University of Texas at Austin, Dec. 1984.
6. I. Sanchez-Salinero. *Analytical Investigation of Seismic Methods Used for Engineering Applications*. Ph.D. dissertation. The University of Texas at Austin, Dec. 1986.
7. J. C. Sheu, K. H. Stokoe, II, J. M. Roesset, and W. B. Hudson. Applications and Limitations of the Spectral-Analysis-of-Surface-Waves Method. *Research Report 437-3F*. Center for Transportation Research, The University of Texas at Austin, 206 pp.
8. R. White, W. R. Hudson, A. H. Meyer, and K. H. Stokoe, II. Design and Construction of a Rigid Pavement Research Facility. *Research Report 355-1*. Center for Transportation Research, The University of Texas at Austin, 121 pp.
9. S. Nazarian, K. H. Stokoe, II and R. C. Briggs. Nondestructively Delineating Changes in Modulus Profiles of Secondary Roads. In *Transportation Research Record 1136*, TRB, National Research Council, Washington, D.C., 1987.
10. S. Nazarian, K. H. Stokoe, II, R. C. Briggs, and R. Rogers. Determination of Pavement Layer Thicknesses and Moduli by SASW Method. In *Transportation Research Record 1196*, TRB, 1988.
11. J. C. Sheu, G. J. Rix and K. H. Stokoe, II. Rapid Determination of Modulus and Thickness of Pavement Surface Layer. Presented at the Transportation Research Board Annual Meeting, 1988.
12. F. E. Richart, Jr., J. R. Hall, Jr., and R. D. Woods. *Vibrations of Soils and Foundations*. Prentice-Hall, Inc., Englewood Cliffs, N.J., 1970.

Publication of this paper sponsored by the Committee on Pavement Monitoring, Evaluation, and Data Storage.